Title
Quenched magnetic moment in Mn-doped amorphous Si films

Journal
Physical Review B, 77(7)

ISSN
2469-9950

Authors
Zeng, Li
□□
Helgren, E
et al.

Publication Date
2008-02-15

DOI
10.1103/physrevb.77.073306

Peer reviewed

Quenched magnetic moment in Mn-doped amorphous Si films

Li Zeng (曾立)*
Materials Science and Engineering Program, University of California, San Diego, La Jolla, California 92093, USA

E. Helgren, M. Rahimi, and F. Hellman
Department of Physics, University of California, Berkeley, Berkeley, California 94720, USA

R. Islam and B. J. Wilkens
Center for Solid State Science, Arizona State University, Tempe, Arizona 85287, USA

R. J. Culbertson and David J. Smith
Department of Physics, Arizona State University, Tempe, Arizona 85287, USA

(Received 22 October 2007; published 19 February 2008)

The absence of a Mn local moment was observed in Mn-doped amorphous silicon (a-Mn_xSi_{1-x}) films. The magnetic susceptibility obeys the Curie-Weiss law for a wide range of x (5×10^{-3} up to 0.175) but with extremely small moment. Magnetization measurements suggest that this behavior occurs because only a small percentage of Mn (Mn^{2+} states with $J=S=5/2$) contribute to the magnetization. Thus, the magnetic moments are quenched for the majority of Mn atoms, contrary to the general belief of the existence of a localized Mn moment in Si. X-ray absorption spectroscopy suggests that the quenching of Mn moments is attributed to the formation of an itinerant but Anderson-localized impurity band, forming at x as low as 5×10^{-3}.

DOI: 10.1103/PhysRevB.77.073306 PACS number(s): 71.55.Cn, 71.23.−k, 72.20.−i, 75.50.Pp

Magnetic moments in semiconductors are important for spin electronics and for fundamental studies of interactions between magnetic and charge degrees of freedom, such as in Mn-doped GaAs (Ref. 1) and vacancy-doped Gd_3S_4.[2] In these crystalline magnetic semiconductors, carrier-induced magnetic ordering, large magnetotransport effects, or magnetic field-tuned metal-insulator (M-I) transitions were observed as a consequence of large moment-carrier interactions. Similar effects were discovered in Gd-doped amorphous Si (a-Gd_xSi_{1-x}) and Ge,[3] including Ruderman-Kittel-Kasuya-Yosida–induced spin-glass (SG) freezing,[3,4] enormous negative magnetoresistance (MR) [$\sim-10^5$ at 1 K (Ref. 5)] and an M-I transition driven by magnetic field, providing evidence for strong local moment-carrier interactions.[3,6] The coexistence of well-defined magnetic moments, charge carriers, and strong moment-carrier interactions is important prerequisites for magnetically doped semiconductors.

Mn-doped crystalline Si (c-Si) and Ge have been the focus of recent studies as potential spintronics materials.[7–13] However, the observed ferromagnetism is controversial and seems to be extrinsic in origin, being attributed to nanocrystallites[13] or chemical inhomogeneity,[11] due to the extremely low thermodynamic solubility of Mn in c-Si ($x\sim10^{-7}$).

We have prepared homogeneous Mn-doped amorphous Si (a-Si) to address the issue of the intrinsic magnetic state as well as to study the moment-carrier interactions. High quality e-beam-evaporated a-Si consisting of a continuous random network[14] of tetrahedrally bonded Si atoms possesses a local chemical environment similar to that of c-Si. Moreover, lower growth temperatures and the forgiving nature of the amorphous structure are conducive to homogeneous doping. Therefore, since charge and spin states are most sensitive to the local environment, Mn moments existing in c-Si should also be observable in a-Si.

The existence of a significant Mn moment in Si, key to ferromagnetic ordering, is predicted by the early model developed by Ludwig and Woodbury (the LW model)[15] for isolated Mn in c-Si, as well as by more recent mean-field theory (Zener model)[16] and first-principles calculations[17,18] in the dilute doping range ($x\sim10^{-2}$). The s-d exchange interaction is expected to be larger than s-f due to the delocalized nature of the $3d$ moment compared to the $4f$ moment. Thus, a local Mn moment in Si would be expected to lead to even larger MR than seen in a-Gd_xSi_{1-x}. Therefore, it is intriguing that the few reports on magnetotransport of Mn-implanted a-Si samples (a-Si_{1-x}:Mn_x, $x\sim0.07-0.22$) showed no large negative MR effect; magnetic properties were not reported.[19–21]

In this Brief Report, we describe a systematic magnetization and magnetotransport study on Mn-doped a-Si (a-Mn_xSi_{1-x}) films (where x ranges from 5×10^{-3} to 0.175), covering both the dilute region and the M-I transition region. Films were grown by e-beam coevaporation from Si and Mn sources onto substrates held near room temperature under ultrahigh-vacuum conditions (base pressure of $\sim8\times10^{-10}$ Torr). *In situ* thickness monitors were used to precisely control the real-time Mn and Si flux to achieve uniform doping profiles as well as the desired Mn concentrations. The resulting films have a more homogeneous and uniform Mn distribution compared to implanted samples, providing a better platform to probe the intrinsic Mn magnetic properties in Si. Film compositions and the absence of oxygen impurities inside the films were established by Rutherford backscattering (RBS) using the oxygen-resonance energy to enhance O sensitivity. No clustering or crystalline phases were observed by high-resolution cross-sectional transmission electron microscopy (HR-XTEM) down to 2 nm, as shown in Fig. 1(a). There are a few regions with diameters of $\leqslant2$ nm which show slight suggestions of poorly defined lattice fringes, but digital diffractograms show typi-

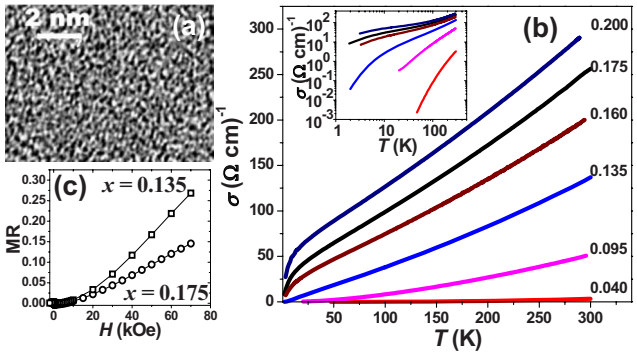

FIG. 1. (Color online) (a) HR-XTEM picture shows homogeneous amorphous microstructure for a typical a-Mn_xSi_{1-x} film. (b) σ_{dc} vs T for a-Mn_xSi_{1-x} measured by four-point probe method on lithographically defined Hall ball geometry. Inset: same data on log-log scale to show clearly insulating behavior for $x=0.04$, 0.095, and 0.135. (c) MR vs H for the $x=0.135$ and $x=0.175$ samples.

cal amorphous ring patterns. Further material characterization details are given in Refs. 14 and 22. Magnetic and magnetotransport measurements were made with a superconducting quantum interference device magnetometer.

For the lowest doping levels, measurements show that the total atomic number density (n_{total}) was comparable to that of c-Si, indicating good quality of the a-Si matrix. n_{total} increased linearly with Mn doping x and agreed with a calculated n_{total} assuming all Mn were interstitial without changing the a-Si matrix density, suggesting that the Mn atoms acted like interstitial Mn (Mn_I) in a-Mn_xSi_{1-x} (and therefore, located at sites with large Si coordination numbers and low symmetry). Substitutional Mn (Mn_{Si}) on the other hand would have kept n_{total} constant and close to the pure a-Si density.

Figure 1(b) shows the T dependence of dc conductivity $\sigma(T)$ for different x. $\sigma(T)$ increases monotonically with x, indicating that Mn is an effective dopant. A concentration-tuned M-I transition is observed; samples are insulating for $x \leqslant 0.135$, whereas they are metallic for higher x.[23] Based on the low temperature $\sigma(T)$, the 0.135 sample is very close to x_c but slightly on the insulating side. This result is in agreement with $x_c=0.137$ found in Mn-implanted a-Si samples.[21] Magnetotransport properties were measured for one sample on the insulating side ($x=0.135$) and one sample on the metallic side ($x=0.175$). A small positive MR $\left(=\frac{\rho(H)-\rho(0)}{\rho(H)}\right)$ was found down to 2 K at $H=7$ kOe for both samples, as shown in Fig. 1(c): 27% and 16% for $x=0.135$ and $x=0.175$, respectively. No negative MR was observed in any sample. The negative MR found in Ref. 19 was attributed to magnetic clusters.

Figure 2(a) shows the magnetization per Mn (M) vs H at 2 K for various x, assuming that all Mn contribute equally. Film signals were very small, less than the diamagnetic response from the SiN_x coated Si substrate. Therefore, the substrate background contribution was carefully measured and subtracted, as was an undoped a-Si control sample prepared using the same Si evaporation batch. The resulting sample magnetization showed no hysteresis loop at any temperature down to 2 K. Figure 2(a) shows that M decreased very

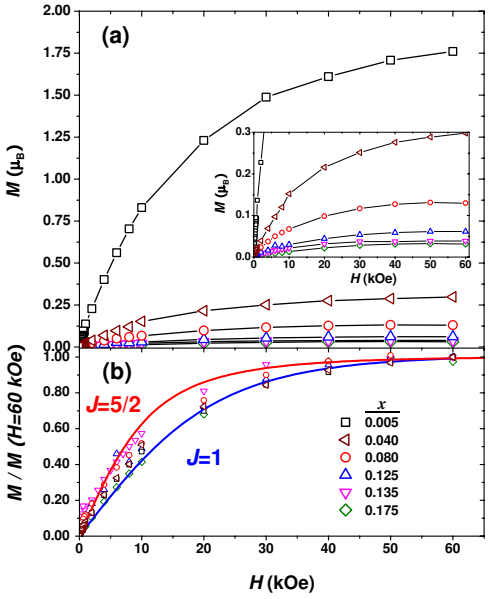

FIG. 2. (Color online) (a) Magnetization per Mn atom in units of μ_B vs H for different Mn concentrations at 2 K, assuming all Mn equally contribute. Inset: same data on expanded scale. Lines are guides to the eye. (b) Normalized M vs H for various compositions x at 2 K. Lines show Brillouin function for $J=S=5/2$ and $J=S=1$ (the two states suggested for interstitial Mn in Si) for comparison.

quickly with increasing x, but all curves scaled well to the Brillouin function for free magnetic ions when normalized to the high field value, as shown in Fig. 2(b). The values of M at 6 kOe were within 2% of the saturation moment according to the Brillouin function and is used later to calculate the saturation moment per Mn (p_{sat}).

Both the zero-field-cooled (ZFC) and the field-cooled (FC) magnetic susceptibilities $[\chi_{ZFC,FC}(T)=M(T)/H]$ were recorded in a dc magnetic field of 10 kOe. The diamagnetic background from the substrate was again subtracted. The resulting net ZFC and FC data are identical and follow the Curie-Weiss (CW) law very closely with a very low CW temperature ($|\theta|<2$ K). For $x=0.04$, which had the largest raw magnetic signal, $\chi_{ZFC,FC}(T)$ was also determined using smaller fields ($H=1000$ and 350 Oe). 10 kOe is a large field for measuring χ and the reduction in χ from its initial value is ~20%, leading to a 10% underestimation of the effective moment (p_{eff}). This high field is necessary to obtain reliable sample signals (strongly T dependent) above the diamagnetic background (negligible T dependence) for our samples. No ferromagnetic or SG states were observed in the temperature range of 2–40 K. Above 40 K, the error bars were large due to the small signal. In order to probe further for possible antiferromagnetic (AFM) or spin glass states, the thermoremanent moment (TRM) was also measured by cooling the sample in a 70 kOe field and then measuring during heating in zero field from 1.9 to 380 K: no significant signal was obtained. These results indicate that samples are purely paramagnetic.

Figure 3 shows the Mn concentration dependence of p_{sat} (M at $T=2$ K, $H=6$ T), as described previously, and of p_{eff} deduced from the CW fitting constant $A=n_{Mn}p_{eff}^2\mu_B^2/3k_B$ (n_{Mn}: Mn number density). Both p_{eff} and p_{sat} decrease

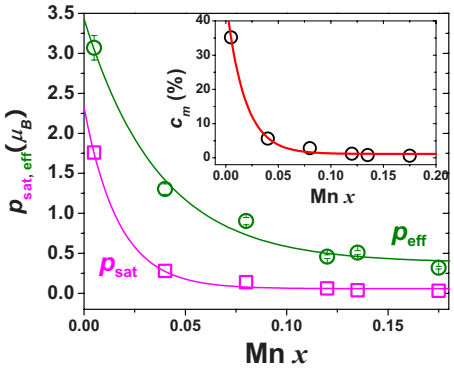

FIG. 3. (Color online) p_{eff} (from $A=n_{\mathrm{Mn}}p_{\mathrm{eff}}^2\mu_B^2/3k_BT$) and p_{sat} [from $M(H=60\ \mathrm{kOe})=n_{\mathrm{Mn}}p_{\mathrm{sat}}$] with different n_{Mn} for each x. Lines are guides to the eye. Inset shows the percentage (c_m) of magnetic centers as a function of x.

sharply from $x=5\times10^{-3}$ to $x=0.04$, becoming very small and negligible with increasing x.

The small magnetization (p_{sat} and p_{eff}) of all samples strongly suggests that only a very small percentage of Mn atoms are magnetically active. Electron spin resonance (ESR) results suggest Mn is in a pure spin state ($g=2$). According to the LW model, there are two known $\mathrm{Mn_I}$ with a quenched orbital moment: $\mathrm{Mn_I}^{2+}$ ($3d^5$, $J=S=5/2$) and $\mathrm{Mn_I}^{-}$ ($3d^8$, $J=S=1$). Instead of assuming all Mn contribute equally (as done above to determine p_{sat} and p_{eff}), the following equations can be solved assuming various fixed J values:

$$p_{\mathrm{sat}} = c_m g J, \tag{1}$$

$$A = \frac{c_m n_{\mathrm{Mn}} (p_{\mathrm{eff}}^m)^2 \mu_B^2}{3k_B}, \tag{2}$$

where p_{sat} and A are experimentally determined as previously mentioned. Equation (1) gives c_m, the percentage of magnetically active Mn. Substituting c_m into Eq. (2), we obtain a new effective moment (denoted as p_{eff}^m) based on $c_m n_{\mathrm{Mn}}$ instead of n_{Mn}, as previously assumed. For a simple paramagnetic state, p_{eff}^m should equal to $g\sqrt{J(J+1)}$ [the same J as in Eq. (1)]. Table I shows that the resulting p_{eff}^m for $J=5/2$ is in excellent agreement with the calculated effective moment ($5.9\mu_B$) within experimental errors [$\sim$10% underestimation of p_{eff}^m comes from determining $\chi(T)$ by using a 10 kOe field, as discussed previously]. This analysis does not work for the $\mathrm{Mn_I}^{-}$ with $J=1$. This provides strong evidence that $\mathrm{Mn_I}^{2+}$ ($3d^5$, $J=S=5/2$) is the magnetically active state, but only accounts for a small percentage of the n_{Mn} (e.g., $c_m=35.2\%$ and 0.6% for $x=5\times10^{-3}$ and 0.175, respectively).

Using $J=5/2$, we plot c_m vs x (Fig. 3, inset). Its rapid decrease explains the low values of p_{sat} and p_{eff} in the main plot. The product of x and c_m (listed in Table I), which gives the atomic concentration of $\mathrm{Mn_I}^{2+}$, is found to be a small constant value, on the order of 10^{-3}, suggesting a constant limit for Mn ions with $J=5/2$ local moments. Above this limit, there is no increase in the number of Mn moments; the added Mn atoms contribute to the transport properties only. This is in sharp contrast to the previously studied magnetically doped system a-$\mathrm{Gd}_x\mathrm{Si}_{1-x}$, which had a SG ground state and showed enormous negative MR.[14] These phenomena in a-$\mathrm{Gd}_x\mathrm{Si}_{1-x}$ are only consistent with each Gd acting as an electron dopant as well as having a large local moment. In contrast, a-$\mathrm{Mn}_x\mathrm{Si}_{1-x}$ behaves like a typical nonmagnetic disordered electronic system with small positive MR.[23]

TABLE I. Sample atomic concentration, magnetically active percentage, effective moment, atomic concentration of magnetic centers, and effective to atomic moment ratio.

x[a]	c_m[b] (%)	p_{eff}^m[c] (μ_B)	xc_m[d] ($\times10^{-3}$)
0.005	35.2	5.2	1.76
0.040	5.6	5.5	2.24
0.080	2.8	5.4	2.24
0.120	1.2	4.1	1.44
0.135	0.8	5.8	1.08
0.175	0.6	4.0	1.05

[a]Mn doping concentration from RBS: a-$\mathrm{Mn}_x\mathrm{Si}_{1-x}$.
[b]Magnetically active percentage from Eq. (1) for $J=5/2$.
[c]Effective moment from Eq. (2) for $J=5/2$.
[d]Atomic concentration of Mn^{2+} in a-Si.

$\mathrm{Mn_I}$ in a-Si is believed to always have a local moment.[15–18,24,25] This should be the same in a-Si since the Mn spin and charge states should mainly depend on local environment. It is possible, but unlikely, that Mn moments exist but are completely canceled out by AFM interactions since AFM ordering is not robust to disorder so AFM interactions between local moments should lead to a magnetically frozen state, such as a SG phase (with T_f) or a clustered SG (with blocking temperature T_B), which would show magnetic hysteresis (differences between the FC and the ZFC states) and TRM. The CW behavior of our samples is reliably measured up to 40 K for x up to 0.175. The known concentrated SG a-MnSi ($x=0.5$) has a T_f only at 22 K,[26] and T_f (T_B) should decrease with decreasing magnetic concentration x. The crystalline MnSi compound has a magnetic ordering temperature ($T_C=30$ K). Above T_f or T_C, in the paramagnetic states, they have comparable p_{eff} of $2.2\mu_B$ and $2.6\mu_B$ for c-MnSi and a-MnSi, respectively, due to similar local environment and short-range order;[27] both of these states would give significantly larger $\chi(T)$ than that observed in a-$\mathrm{Mn}_x\mathrm{Si}_{1-x}$.

Another possible source for vanishing Mn moment with increasing x is the formation of local AFM clusters. Mn clusters in a-Si (which would be invisible in HR-XTEM), such as Mn dimers or trimers, could potentially have an AFM configuration and zero moment. However, such complexes have never been observed in Si experimentally to the best of our knowledge and are theoretically found to have higher energy than FM-coupled configurations[25,28] which would result in an *enhanced* p_{eff}. Only the neutral charge state of $\mathrm{Mn_I}$ favors AFM coupling in Si,[28] which would not contribute to electrical transport, contrary to observation. $\mathrm{Mn_4}^0$ (Ref. 15) and [$\mathrm{Mn_{3I}}^0$-$\mathrm{Mn_I}^-$] (Ref. 29) clusters have large S values. Therefore, pairs and polyclustering (up to four Mn atoms) are unlikely to be the reason for the absence of magnetism in

a-Mn_xSi_{1-x}. Existence of metallic Mn or Mn-rich clusters of larger scale are not supported by the HR-XTEM results and the atomic density analysis. Therefore, AFM clusters are unlikely to be the cause of the small magnetic moment.

We propose that the lack of Mn magnetization in a-Si is due to the formation of bandlike itinerant states. The existence of itinerant states in insulating samples is explained by Anderson localization in strongly disordered amorphous materials. States in the itinerant band are localized due to disorder when $x \leqslant x_c$ (the localized length depends on x, but is generally much longer than an interatomic distance) and delocalized when $x > x_c$. These localized itinerant states have no magnetic moment. For some metallic Mn silicides, such as crystalline Mn_4Si_7, itinerant magnetism is found with tiny p_{eff} and p_{sat}: $0.365\mu_B$ and $0.012\mu_B$, respectively.[30] The symmetry at the Mn site in this compound is low (space group $P\bar{4}c2$) and may be a better representation of the local environment of Mn in a-Mn_xSi_{1-x}. It is also possible, given the usual strong s-d exchange interactions, that a Kondo effect plays a role in reducing the magnetic moment.

The model of a localized itinerant state is supported by x-ray absorption spectroscopy (XAS) studies. Samples with $x \geqslant 0.04$ show two broad Mn L edges, which resemble the spectra for transition metals with delocalized d bands. In the $x=5\times10^{-3}$ sample, mixed electronic states are observed. Analysis shows that its Mn L_3 edge can be decomposed into two separate spectra: one with the broad edges found in the high Mn doping samples, and the other with Mn^{2+} atomic multiplet structures, consistent with our magnetic data, indicating 35% Mn^{2+}, $S=5/2$ centers. The broad absorption edges are therefore assigned to nonmagnetic Mn states and are characteristic of strong covalency and band formation.

In conclusion, an unexpected quenched Mn moment state has been observed in Mn-doped a-Si, forming at the lowest x studied (5×10^{-3}), which is not predicted by any existing model for transition metal dopants in Si. This result explains why MR for a-Mn_xSi_{1-x} is positive and small, with typical values for disordered nonmagnetic electronic systems, unlike the enormous negative MR found in a-Gd_xSi_{1-x}. The nonmagnetic state is most likely due to the formation of an impurity band, subject to localization effects. The existence of the itinerant state is related to the local short-range Mn-Si covalency and may explain why the quest for discovering intrinsic dilute magnetic semiconductor based on Mn-doped Si has not been successful compared to Mn-doped III-V semiconductors. Our results also suggest that there is a concentration limit ($x \sim 10^{-3}$) where the LW model for Mn in Si is no longer valid due to formation of bands.

We thank S. Lofland for ESR, E. Arenholz, E. Cruz, and C. Piamonteze for XAS, and D. R. Queen, N. Spaldin, A. J. Freeman, Hua Wu, and M. Scheffler for useful discussions. We acknowledge use of facilities in the LeRoy Eyring Center for Solid State Science at ASU. This research was supported by NSF DMR-0505524.

*lzeng@ucsd.edu

[1] H. Ohno, Science **281**, 951 (1998).
[2] S. von Molnar, A. Briggs, J. Flouquet, and G. Remenyi, Phys. Rev. Lett. **51**, 706 (1983).
[3] E. Helgren, F. Hellman, L. Zeng, N. Sinenian, R. Islam, and D. J. Smith, Phys. Rev. B **76**, 184440 (2007).
[4] F. Hellman, D. R. Queen, R. M. Potok, and B. L. Zink, Phys. Rev. Lett. **84**, 5411 (2000).
[5] F. Hellman, M. Q. Tran, A. E. Gebala, E. M. Wilcox, and R. C. Dynes, Phys. Rev. Lett. **77**, 4652 (1996).
[6] P. Xiong, B. L. Zink, S. I. Applebaum, F. Hellman, and R. C. Dynes, Phys. Rev. B **59**, R3929 (1999).
[7] Y. D. Park, A. T. Hanbicki, S. C. Erwin, C. S. Hellberg, J. M. Sullivan, J. E. Mattson, T. F. Ambrose, A. Wilson, G. Spanos, and B. T. Jonker, Science **295**, 651 (2002).
[8] S. Cho, S. Choi, S. C. Hong, Y. Kim, J. B. Ketterson, B.-J. Kim, Y. C. Kim, and J.-H. Jung, Phys. Rev. B **66**, 033303 (2002).
[9] M. Bolduc, C. Awo-Affouda, A. Stollenwerk, M. B. Huang, F. G. Ramos, G. Agnello, and V. P. LaBella, Phys. Rev. B **71**, 033302 (2005).
[10] Y. H. Kwon, T. W. Kang, H. Y. Cho, and T. W. Kim, Solid State Commun. **136**, 257 (2005).
[11] J.-S. Kang *et al.*, Phys. Rev. Lett. **94**, 147202 (2005).
[12] S. Ma, Y. Sun, B. Zhao, P. Tong, X. Zhu, and W. Song, Solid State Commun. **140**, 192 (2006).
[13] S. Zhou *et al.*, Phys. Rev. B **75**, 085203 (2007).
[14] L. Zeng, E. Helgren, F. Hellman, R. Islam, and D. J. Smith, Phys. Rev. B **75**, 184404 (2007).
[15] G. W. Ludwig and H. H. Woodbury, Phys. Rev. Lett. **5**, 98 (1960).
[16] T. Dietl, H. Ohno, F. Matsukura, J. Cibert, and D. Ferrand, Science **287**, 1019 (1998).
[17] A. Stroppa, S. Picozzi, A. Continenza, and A. J. Freeman, Phys. Rev. B **68**, 155203 (2003).
[18] H. Weng and J. Dong, Phys. Rev. B **71**, 035201 (2005).
[19] A. I. Yakimov, T. Wright, C. J. Adkins, and A. V. Dvurechenskii, Phys. Rev. B **51**, 16549 (1995).
[20] A. I. Yakimov, A. V. Dvurechenskii, C. J. Adkins, and V. A. Dravin, J. Phys.: Condens. Matter **9**, 499 (1997).
[21] A. I. Yakimov and A. V. Dvurechenskii, JETP Lett. **65**, 354 (1997).
[22] L. Zeng, E. Helgren, F. Hellman, R. Islam, D. J. Smith, and J. W. Ager III, Phys. Rev. B **75**, 235450 (2007).
[23] P. A. Lee and T. V. Ramakrishnan, Rev. Mod. Phys. **57**, 287 (1985).
[24] H. Wu, M. Hortamani, P. Kratzer, and M. Scheffler, Phys. Rev. Lett. **92**, 237202 (2004).
[25] Hua Wu and Matthias Scheffler (private communication).
[26] J. J. Hauser, F. S. L. Hsu, G. W. Kammlott, and J. V. Waszczak, Phys. Rev. B **20**, 3391 (1979).
[27] R. W. Cochrane, J. O. Strom-Olsen, and J. P. Rebouillat, J. Appl. Phys. **50**, 7348 (1979).
[28] F. Bernardini, S. Picozzi, and A. Continenza, Appl. Phys. Lett. **84**, 2289 (2004).
[29] J. Kreissl, W. Gehlhoff, and H. Vollmer, Phys. Rev. B **49**, 10307 (1994).
[30] U. Gottlieb, A. Sulpice, B. Lambert-Andron, and O. Laborde, J. Alloys Compd. **361**, 13 (2003).